

Retraction

Retracted: Structural Classification of Basalt FRP at High Temperatures

Advances in Materials Science and Engineering

Received 26 December 2023; Accepted 26 December 2023; Published 29 December 2023

Copyright © 2023 Advances in Materials Science and Engineering. This is an open access article distributed under the Creative Commons Attribution License, which permits unrestricted use, distribution, and reproduction in any medium, provided the original work is properly cited.

This article has been retracted by Hindawi, as publisher, following an investigation undertaken by the publisher [1]. This investigation has uncovered evidence of systematic manipulation of the publication and peer-review process. We cannot, therefore, vouch for the reliability or integrity of this article.

Please note that this notice is intended solely to alert readers that the peer-review process of this article has been compromised.

Wiley and Hindawi regret that the usual quality checks did not identify these issues before publication and have since put additional measures in place to safeguard research integrity.

We wish to credit our Research Integrity and Research Publishing teams and anonymous and named external researchers and research integrity experts for contributing to this investigation.

The corresponding author, as the representative of all authors, has been given the opportunity to register their agreement or disagreement to this retraction. We have kept a record of any response received.

References

- [1] S. Vummadisetti, S. R. Pasalapudi, S. K. Gottapu, K. K. Goriparthi, and A. Batu, "Structural Classification of Basalt FRP at High Temperatures," *Advances in Materials Science and Engineering*, vol. 2021, Article ID 6917471, 9 pages, 2021.

Research Article

Structural Classification of Basalt FRP at High Temperatures

Sudhir Vummadiseti ¹, Sesa Ratnam Pasalapudi ², Santosh Kumar Gottapu ³,
Kranthi Kumar Goriparthi ³ and Areda Batu ⁴

¹Department of Civil Engineering, Vignan's Institute of Information Technology (A), Duvvada, Visakhapatnam 530049, India

²Department of Civil Engineering, Gayatri Vidya Parishad, Rushikonda, Visakhapatnam 530045, India

³Department of Civil Engineering, Gayatri Vidya Parishad College of Engineering (A), Madhurawada, Visakhapatnam 530048, India

⁴Department of Chemical Engineering, College of Biological and Chemical Engineering, Addis Ababa Science and Technology University, Addis Ababa, Ethiopia

Correspondence should be addressed to Areda Batu; areda.batu@aastu.edu.et

Received 6 August 2021; Revised 23 August 2021; Accepted 27 August 2021; Published 13 September 2021

Academic Editor: Samson Jerold Samuel Chelladurai

Copyright © 2021 Sudhir Vummadiseti et al. This is an open access article distributed under the Creative Commons Attribution License, which permits unrestricted use, distribution, and reproduction in any medium, provided the original work is properly cited.

In this study, two different temperatures are considered to verify the mechanical response of basalt fiber-reinforced polymer specimens. Initially, fibers are subjected to 300°C temperature for 4 hours and 600°C temperature for 2 hours in an electrical muffle furnace effectively. Later, laminates were prepared with these fibers and machined into test strips to verify their mechanical properties by conducting tensile and flexural tests. These laminates were compared with specimens prepared with normal fibers, i.e., fibers without temperature treatment. Moreover, the ductility and elastic behavior of the basalt fiber-laminated specimens are studied to figure out the possible structural applications. The residual stress of specimens subjected to 300°C temperature under tensile loading is about 84%, whereas for 600°C temperature, it is only 13% of maximum stress. A similar trend has been observed for specimens tested under flexural loading condition. Hence, it is concluded that the basalt fiber-reinforced polymer laminate can withstand and depict satisfactory results up to 300°C elevated temperature irrespective of time.

1. Introduction

Ductility is the capacity of a structural member to undertake large inelastic deformations without notable loss of strength or stiffness. Due to ductility, structures or materials can absorb energy by deforming into an inelastic range under the application of force. In other words, it is the ability to withstand plastic deformation before fracture which can be defined as the ratio of the ultimate deformation at an assumed collapse point to the yield deformation. For resistance to earthquake forces, the structure, elements, and connections shall be designed to have ductile failure to avoid sudden collapse. However, ductility is hard to achieve in many structural members such as deep beams, pile caps, and corbels. Since such members tend to fail mostly in the shear mode, the assumptions of the linear-elastic flexural theory and pure bending theory are not valid. These members require special considerations for design and

detailing. Therefore, in order to achieve ductility, many design methodologies like Strut-and-Tie model and materials such as admixtures, plasticizers, and fibers are adopted. Moreover, with the increase in fire-related disasters around the world, the importance of fire-resistant construction is escalating.

In recent decades, many researchers [1–11] have studied the properties and applicability of basalt fiber in structural members due to its high temperature resistance, high durability, high elastic strength, sustainability, etc. It has been found that satisfactory mechanical and thermal-resistant properties of structural members can be achieved using chopped basalt fibers, basalt fiber-reinforced polymer (BFRP) bars, BFRP sheets, laminates, etc. However, contradictory findings are also available in the literature regarding the residual mechanical strength of basalt fibers subjected to elevated temperature conditions. Therefore, in this work, an attempt has been made to study the mechanical

properties of basalt fibers subjected to various temperature conditions. The chopped fibers could not be tested directly due to the smaller lengths, for which laminates are prepared to test the mechanical properties as per ASTM standards. The basalt fiber samples were elevated to different temperatures, and then, through mechanical testing, the residual stress of fibers was evaluated and compared. Therefore, in recent times, the basalt fibers are of importance in research because of its high mechanical properties, thermal resistance, durability, sustainability, low production cost, etc. Basalt filaments are formed by melting the basalt rock which passes through orifices and pullers over a roller [12]. The economic advantage, lower environmental impact, and higher mechanical strength are achieved because no additives are required to produce these fibers from high-strength basalt rocks. The authors of [12, 13] found that volcanic magma crystallizes to basalt with very low water content at the time of crystallization. Basalt rocks are the partial melting products of primitive rocks such as garnet peridotite. Basalt consists of minerals such as plagioclase and clinopyroxene along with olivine, nepheline, melilite, hypersthene, quartz, etc. Based on the original rock used, the produced fibers may exhibit different mechanical and chemical properties. Soares et al. [14] stated that acidic basalt which contains more than 46% of SiO_2 is suitable for production of basalt fiber because in order to develop glass network, high silica content is necessary. As stated earlier, basalt fibers are available with different chemical compositions containing 51.56–57.5% SiO_2 , 16.9–18.2% Al_2O_3 , 5.2–7.8% CaO , 1.3–3.7% MgO , 2.5–6.4% Na_2O , 0.8–4.5% K_2O , 4.0–9.5% Fe_2O_3 , etc.

Investigation was performed on temperature resistance of basalt fibers which generally has an operational temperature range from -200°C to 800°C [15]. Basalt fibers perform much better than glass fibers as the temperature range of basalt fibers is -269°C to 700°C as compared to glass fibers whose temperature range is from -60°C to 500°C [16]. Most of the studies show that basalt fibers perform very efficiently at high temperatures. However, contradictory results are found in different literature studies regarding the residual mechanical strength of basalt fibers subjected to elevated temperature conditions. The authors of [16] found that with the increase of time of exposure and elevated temperature up to 300°C , the strength of basalt fibers increased up to 19.1%. Also, 32.8% reduction of strength is observed in similar testing conditions [17]. Zollo et al. [16] explained that the reformation of fiber structure around the nucleating agents led to the thermal stability of the fibers. However, Arvo Ivar and Bjorklund [17] described from SEM and XRD analysis that the short-order structure of basalt fibers decreased in size which led to reduction in tensile strength. A lot of research was performed on functionally graded hybrid composite materials, and parametric study has also been performed on these novel layups [18–22]. This layup can be applied in case of basalt fibers also. Therefore, it is necessary to analyze residual mechanical strength of the basalt fiber specimens subjected to elevated temperatures because such variations occur due to the change in the

crystalline structure of the fiber which is mainly governed by the presence of iron oxides.

2. Experimental Methods

2.1. Procedure

2.1.1. Tensile Properties of BFRP Specimens. The in-plane tensile properties of polymer matrix composite materials reinforced with high-modulus fibers can be determined as per ASTM D 3039/D3039M [23]. Monotonically tensile load is applied on the flat strip of the material with a constant rectangular cross section which is mounted in the grips as shown in Figure 1.

The maximum load carried before failure is the ultimate failure strength of the material. Moreover, if the strain or displacement is monitored, then stress-strain response can be obtained. The speed of test should be controlled at a constant head displacement rate of 2 mm/min or a standard strain rate of 0.01 min^{-1} .

2.1.2. Flexure Properties of BFRP Specimens. Basalt fiber-reinforced polymer (BFRP) specimens were subjected to flexural load under the three-point bending system as shown in Figure 2. Both rigid and semirigid materials in the shape of rectangular bars moulded directly or machined from plates, sheets, or moulded shapes can be tested within the 5% strain limit of the test methods [1].

As shown in Figure 2, a bar of rectangular cross section resting on two supports is loaded at midway where the radius of the support is of minimum 3.2 mm to maximum 1.6 times the specimen depth, whereas the maximum radius of the loading nose is limited to 4 times the specimen depth. The support span-to-depth ratio of 16:1 should be maintained at a strain rate of 0.01 mm/mm/min. The failure occurs at a maximum strain of 5%. The rate of crosshead motion is determined using the following equation:

$$R = \frac{ZL^2}{6D} \quad (1)$$

The flexural strength, chord, secant, or tangent modulus of elasticity and the total work can be measured by calculating the area under the load-deflection curve. If “ r ” is the strain in mm/mm, the mid-span deflection (D) can be calculated using the following equation:

$$D = \frac{rL^2}{6d} \quad (2)$$

2.2. Material Properties

2.2.1. Basalt Fibers. Basalt fibers were acquired from Go Green Products, Chennai, which were of 24 mm length and diameter more than 5 microns (Go Green Products 2018). As per the supplier, the density was 2.6 g/cm^3 , melting point was 1450°C , and they constituted odorless golden shine fibers (Figure 3). Their chemical composition is shown in Table 1.



FIGURE 1: Tensile test of the BFRP specimen with a universal testing machine.

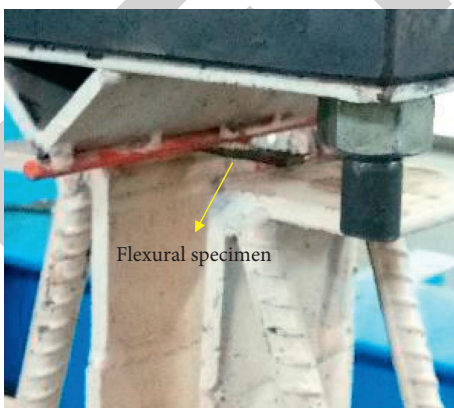


FIGURE 2: Three-point loading for testing of BFRP flexure specimens.

2.2.2. Epoxy and Hardener. An epoxy resin of grade “Resin 691” and a hardener of grade “Reactive Polyamide 140” have been used. The ratio of the resin to hardener is maintained at 9:1 by weight [24]. The mechanical properties of the resin are given in Table 2.



FIGURE 3: Chopped basalt fibers.

TABLE 1: Chemical composition of basalt fibers as provided by the supplier.

Chemical name	Percent
SiO ₂	51.6%–59.3
Al ₂ O ₃	14.6%–18.3
CaO	5.9%–9.4
MgO	3.0%–5.2
Na ₂ O + K ₂ O	3.6%–5.3
TiO ₂	0.8%–2.25
Fe ₂ O ₃ + FeO	9.0%–14.0
Others	0.09%–0.13

TABLE 2: Mechanical properties of Resin 691.

Property	Value
Density (g/cm ³)	2.6
Poisson's ratio	0.32
Tensile strength (MPa)	71
Tensile stiffness (GPa)	3.6
Tensile failure strain (%)	4.0
Glass transition temperature (°C)	91.23
Decomposition temperature (°C)	230

TABLE 3: Thermal properties of the basalt fiber.

Property	Value
Work temperature, °C	–269 to 700°C
Blind temperature, °C	1050°C
Thermal conductivity coefficient (w/m° K)	0.03 to 0.038
Maximum service temperature, °C	650°C
Melting temperature, °C	1350°C
Fire blocker	Upto 1200°C
Coefficient of thermal expansion	$1.4 \times 10^{-6}/^{\circ}$
Specific heat capacity	0.86 J/g.K

The thermal properties of the basalt fiber are significant in the current study. Hence, the properties are depicted in Table 3.



FIGURE 4: Basalt fibers subjected to temperature heating: (a) muffle furnace; (b) fibers removed from muffle furnace after heating.



FIGURE 5: Aluminum sheets used for curing for smooth finishing.



FIGURE 6: Dimensioning and cutting of specimens from the laminates with a DoAll machine.

3. Specimen Preparation

As per ASTM D3039/D3039M [3], five basalt fiber-reinforced (BFRP) specimens of uniform geometry should be prepared. The geometry depends on fiber orientation, gage length, grip type and length, use of tab, etc. At three places in the gage section, width (w) and thickness (h) are calculated to find the average cross-section area (A) from the following equation:

$$A = w \times h. \quad (3)$$

The laminates of size $310 \times 310 \times 2.5 \pm (0.15)$ mm (length \times width \times thickness) are prepared in the mould developed at Advanced Composites Laboratory, BITS, Pilani. The mechanical properties of basalt fibers are characterized

by subjecting them to elevated temperatures of 300°C and 600°C . Initially, the fibers are kept in an electric muffle furnace as shown in Figure 4(a), and the fibers are removed after heating, as shown in Figure 4(b).

The mould of heavy flat metal base plates is used to apply uniform pressure to prepare the laminates, flat aluminum sheets are used for smooth surface finishing, and the outer rectangular blockboard ring is used to maintain the dimension of the laminates, as shown in Figure 5. The matrix consists of the epoxy resin of grade "Resin 691" along with the hardener "Reactive Polyamide 140" at the ratio of 9:1 by weight. The ratio of the fiber to matrix is maintained as 0.6. Since the glass transition temperature of the resin is 91.23°C and decomposition temperature is 230°C only, the laminates are not tested at

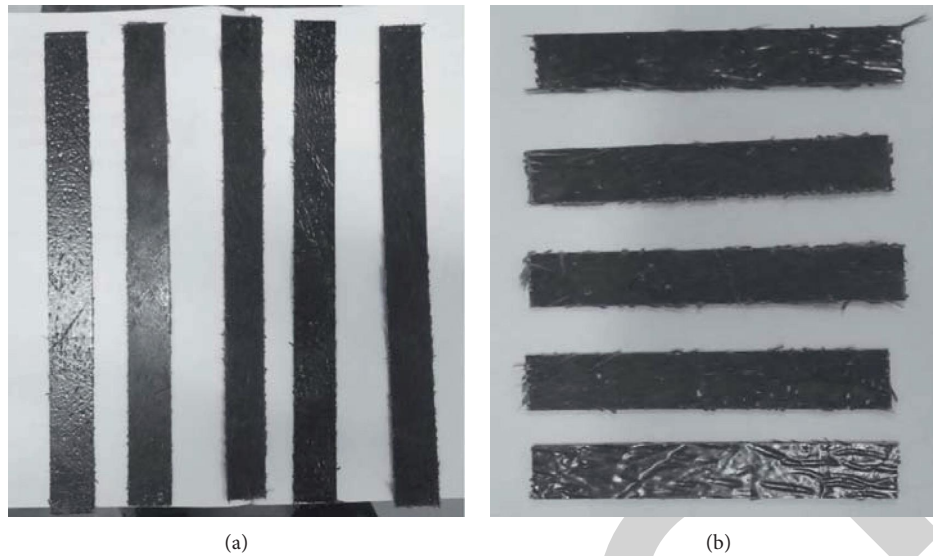


FIGURE 7: Test specimens: (a) tensile and (b) flexural specimens.



FIGURE 8: Failure of the BFRP specimen under tensile loading.

elevated temperatures but only the residual stress of fibers are calculated by preparing the laminates using the resin and hardener. Even though many attempts were made to prepare linearly oriented fiber-reinforced composite plates, due to the smaller length of the fiber and dispersion of epoxy resin, the orientation of fibers in the laminates was considered as randomly distributed. After mixing the fibers with the matrix, the

plates are tightened using screws and kept for minimum 40 hours of conditioning.

After proper conditioning of the laminates, specimens are prepared by cutting using a DoAll cutting machine at Mechanical Workshop, BITS, Pilani, as shown in Figure 6. The tensile specimens of size $250 \times 25 \times 2.5$ mm (length \times width \times thickness) are considered as per Table 2 of ASTM D 3039/D 3039M, and flexure specimens of size 12.7×2.5 mm (width \times thickness) with varying lengths are used to accommodate at least 10% overhanging after maintaining 16 : 1 span-to-depth ratio conforming to ASTM D790 [25].

Three types of specimens have been prepared in this study. One with fibers without any temperature treatment, other with fibers subjected to 300°C elevated temperature, and the last with fibers subjected to 600°C elevated temperature. These three specimens are named as BFRP-I, BFRP-II, and BFRP-III, respectively. Laminates are machined, and all the 5 specimens (both for tensile and flexural tests) are depicted in Figure 7.

The coefficient of variation of the tensile and flexural stress of the specimens tested has been calculated using equation (4) to maintain the quality of work done. The coefficient of variation for all the specimens is not greater than 10% which is considerable:

$$\bar{x} = \sum \frac{x_i}{n} \quad (4)$$

4. Results and Discussion

The BFRP specimens are tested, and the results are discussed as follows.

4.1. Tensile Behavior. The failure of the BFRP specimen tested in a universal testing machine is shown in Figure 8. The type of failure observed was lateral gage middle (LGM)

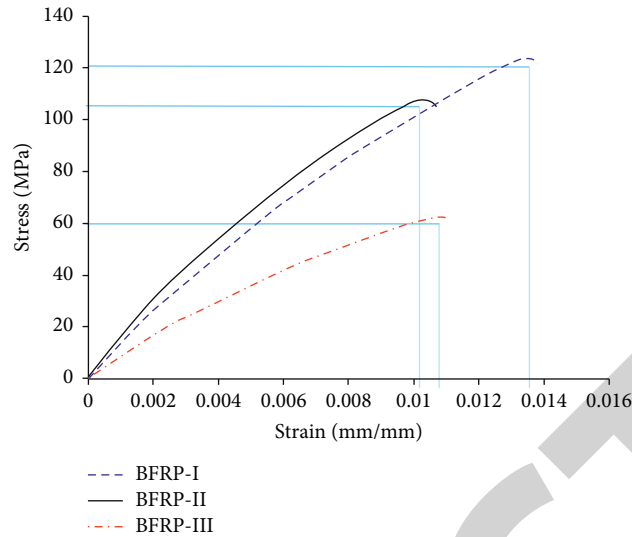


FIGURE 9: Stress-strain response of tensile BFRP specimens.

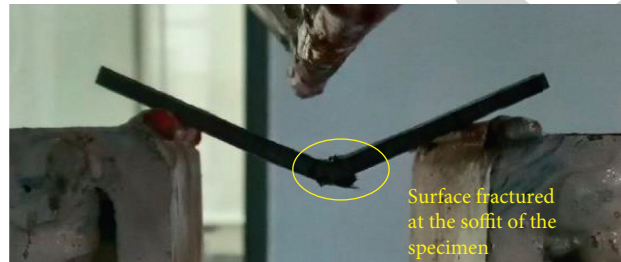


FIGURE 10: Three-point bending test conducted on the BFRP specimen.

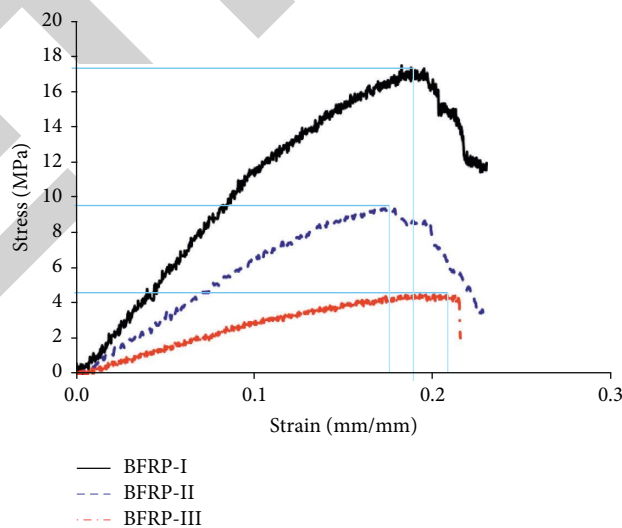


FIGURE 11: Stress-strain response of flexural BFRP specimens tested at room temperature and elevated temperature.

failure since the crack appeared laterally at the mid-position of the specimen. A similar type of failure was observed in all the specimens tested under tensile load.

The stress-strain graphs of BFRP-I, BFRP-II, and BFRP-III are depicted in Figure 9, and the bar charts representing

the maximum stress obtained and the maximum strain obtained at peak stress are also shown in Figure 12.

BFRP-I has obtained the highest tensile stress among other specimens subjected to elevated temperature. It is worth noting that specimens elevated at 600°C have the least tensile stress.

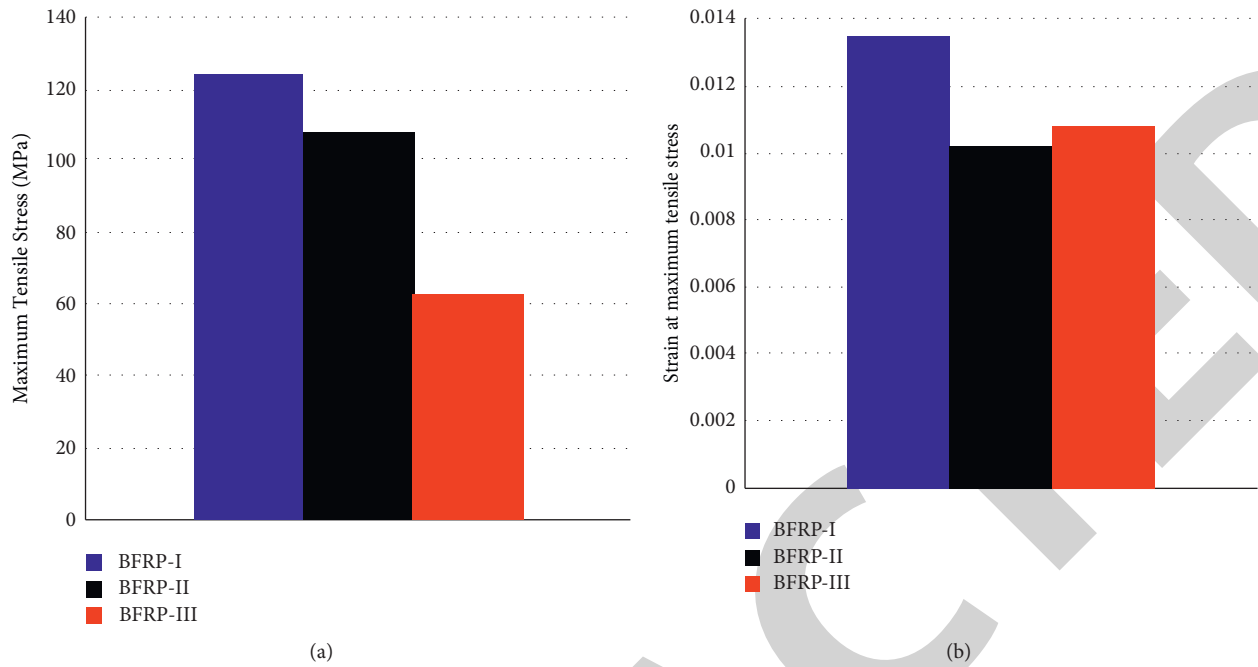


FIGURE 12: Tensile bar charts: (a) maximum stress with respect to specimen; (b) strain at maximum stress obtained.

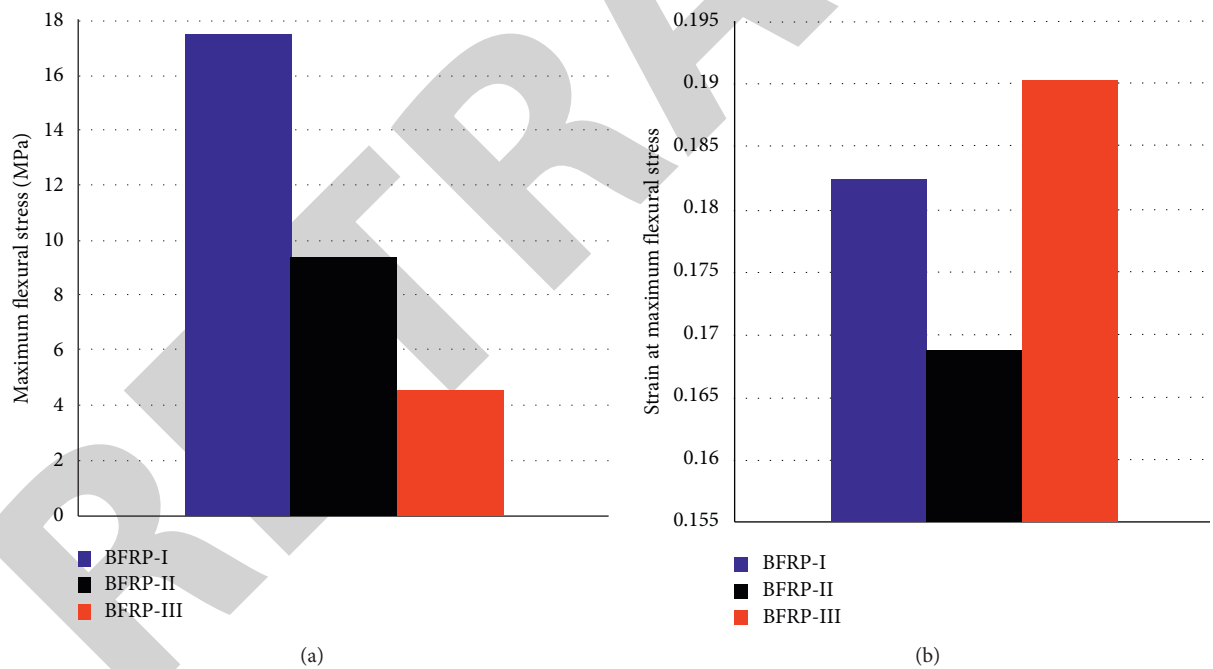


FIGURE 13: Flexure bar charts: (a) maximum stress with respect to specimen; (b) strain at maximum stress obtained.

Hence, it is observed that increase in tensile stress is observed until 300°C temperature. Further increase in temperature leads to decrease in tensile stress. Although the stress is low, temperature-elevated specimens exhibit ductile nature; i.e., the failure of the specimens is not catastrophic.

4.2. Flexural Behavior. The specimens are tested under a three-point bending apparatus as shown in Figure 10. The

soffit of the specimen was fractured upon the application of load at the middle as shown in Figure 10.

The flexural stress-strain graphs are plotted in Figure 11. It is observed that BFRP-I, i.e., the specimen without temperature curing, obtained the highest flexural stress among other specimens. The BFRP-II specimen has higher flexural stress than the BFRP-III specimen. A similar trend has been observed in the case of tensile specimens.

As shown in Figures 12 and 13, the residual tensile stress of basalt fibers elevated to 300°C is around 84%, whereas for 600°C, it is around 13% of maximum stress. However, the strain at maximum stress shows that ductile behavior of the specimen is maintained even at 600°C which signifies that even at higher temperature, the fibers perform quite well in case of serviceability. The reduction of stress due to higher temperature may not be due to change in the crystalline structure of the fibers but also due to poor interlaminar shear strength. The specimens are ductile in nature since none of the specimens collapsed suddenly (see Figures 9 and 11).

Particularly, in comparison with the tensile results, it was discovered that the residual stress of flexure basalt fibers elevated at 300°C is approximately 54% of the maximum stress, while it is approximately 10% of the maximum stress in the case of fibers elevated at 600°C.

The current study's structural applications are diverse. The laminates made of basalt fiber can be used as a direct material or as a retrofitting material. Roof panels, pultruded beams, load bearing I-sections, partition members, pedestrian bridges, railway sleepers, and other structural members made of basalt fibers can be used directly. The basalt fibers can be utilized for column wrapping and slab strengthening by connecting the fiber sheet at the soffit and as near surface mounted members in the case of retrofitting technique. The following are some of the applications for basalt fiber-reinforced polymer laminates. The added benefit of this material, in particular, is that it is thermally resistant.

5. Conclusions

The following conclusions are made from this study:

- (1) Basalt fiber has high tensile strength and modulus of elasticity, making it suitable for use in reinforced composites.
- (2) The electrical insulation of basalt fiber is greater than that of glass fiber.
- (3) The electromagnetic wave has excellent permeability; if a basalt fiber cloth is added to the building's wall, it can produce good shielding for all types of electromagnetic waves.
- (4) The residual stress of basalt fiber decreases, as the temperature increases in case of both tensile and flexural specimens irrespective of time.
- (5) The experiment shows the sustainability and reusability of basalt fiber since at higher temperature, the ductile behavior is maintained and residual stress up to 300°C is still satisfactory.
- (6) With the use of high-temperature-resistant epoxy resin, basalt fibers can be used in fire-resisting constructions very effectively.
- (7) Excellent compatibility with metal, plastic, carbon fiber, and other materials is found. Also, the composite of basalt continuous fiber and various types of resin has a stronger bonding strength than of glass fiber and carbon fiber. In terms of strength,

composites made of continuous basalt fiber are equivalent to E-glass fiber, but elastic modulus has obvious advantages in all types of fibers.

Abbreviations

- A: Area of cross section of the specimen (mm²)
 R: Crosshead motion (mm)
 Z: Rate of straining (mm/mm/min)
 L: Support span (mm)
 d: Depth of the beam (mm)
 r: Strain (mm)
 D: Mid-span deflection (mm)
 w: Width of the specimen (mm)
 h: Thickness of the specimen (mm)
 \bar{x} : Average value of samples
 n: Number of specimens.

Data Availability

The data used to support the findings of this study are included within the article.

Disclosure

This study was performed as part of the employment at Addis Ababa Science and Technology University, Addis Ababa, Ethiopia.

Conflicts of Interest

The authors declare that there are no conflicts of interest.

References

- [1] J. Sim and C. Park, "Characteristics of basalt fiber as a strengthening material for concrete structures," *Composites Part B: Engineering*, vol. 36, no. 6-7, pp. 504-512, 2005.
- [2] S. Carmignato, I. M. De Rosa, F. Sarasini, and M. Valente, "Characterization of basalt fibre reinforced vinylpolyester composite: an overview," in *Proceedings of the 2nd International Conference on Innovative Natural Fiber Composites for Industrial Applications*, Rome, April 2009.
- [3] A. N. Lisakovski, Y. L. Tsybulya, and A. A. Medvedyev, "Yarns of basalt continuous fibers," in *Proceedings of the Fiber Society Spring 2001 Meeting*, pp. 23-25, Raleigh, NC, May 2001.
- [4] J.-M. Park, W.-G. Shin, and D.-J. Yoon, "A study of interfacial aspects of epoxy-based composites reinforced with dual basalt and SiC fibres by means of the fragmentation and acoustic emission techniques," *Composites Science and Technology*, vol. 59, no. 3, pp. 355-370, 1999.
- [5] S. Matkó, P. Anna, G. Marosi et al., "Use of reactive surfactants in basalt fiber reinforced polypropylene composites," *Macromolecular Symposia*, vol. 202, no. 1, pp. 255-268, 2003.
- [6] T. Czigány, "Basalt fiber reinforced hybrid polymer composites," *Materials Science Forum*, vol. 473-474, pp. 59-66, 2005.
- [7] P. I. Bashantnik, V. G. Ovcharenko, and Y. A. Boot, "Effect of combined extrusion parameters on mechanical properties of basalt fiber-reinforced plastics based on polypropylene," *Mechanics of Composite Materials*, vol. 33, no. 6, pp. 600-603, 1997.

- [8] S. Öztürk, "The effect of fibre content on the mechanical properties of hemp and basalt fibre reinforced phenol formaldehyde composites," *Journal of Materials Science*, vol. 40, no. 17, pp. 4585–4592, 2005.
- [9] S. E. Artemenko, "Polymer composite materials made from carbon, basalt, and glass fibres. structure and properties," *Fibre Chemistry*, vol. 35, no. 3, pp. 226–229, 2003.
- [10] J. Jancar, "Effect of interfacial shear strength on the mechanical response of polycarbonate and PP reinforced with basalt fibers," *Composite Interfaces*, vol. 13, no. 8-9, pp. 853–864, 2006.
- [11] L. Qiang, M. T. Shaw, R. S. Parnas, and A.-M. McDonnell, "Investigation of basalt fiber composite aging behavior for applications in transportation," *Polymer Composites*, vol. 27, no. 5, pp. 475–483, 2006.
- [12] Z. Lu and G. Xian, "Resistance of basalt fibers to elevated temperatures and water or alkaline solution immersion," *Polymer Composites*, vol. 39, no. 7, pp. 2385–2393, 2018.
- [13] J. Militký, V. Kovačič, and J. Rubnerová, "Influence of thermal treatment on tensile failure of basalt fibers," *Engineering Fracture Mechanics*, vol. 69, no. 9, pp. 1025–1033, 2002.
- [14] B. Soares, R. Preto, L. Sousa, and L. Reis, "Mechanical behavior of basalt fibers in a basalt-UP composite," *Procedia Structural Integrity*, vol. 1, pp. 82–89, 2016.
- [15] R. Felicetti and P. G. Gambarova, "Effects of high temperature on the residual compressive strength of high-strength siliceous concretes," *ACI Materials Journal*, vol. 95, no. 4, pp. 395–406, 1998.
- [16] R. F. Zollo, "Fiber-reinforced concrete: an overview after 30 years of development," *Cement and Concrete Composites*, vol. 19, no. 2, pp. 107–122, 1997.
- [17] M. Arvo Ivar and F. R. Bjorklund, "Method of reinforcing concrete with fibres," U.S. Patent 4,062,913, issued December 13, 1977.
- [18] S. B. Singh, S. Vummadisetti, and H. Chawla, "Assessment of interlaminar shear strength in hybrid fiber reinforced composites," *Journal of Structural Engineering - SERC*, vol. 46, no. 2, pp. 146–153, 2018.
- [19] S. Vummadisetti and S. B. Singh, "Buckling and postbuckling response of hybrid composite plates under uniaxial compressive loading," *Journal of Building Engineering*, vol. 27, Article ID 101002, 2020.
- [20] S. B. Singh, S. Vummadisetti, and H. Chawla, "Development and characterisation of novel functionally graded hybrid of carbon-glass fibres," *International Journal of Materials Engineering Innovation*, vol. 11, no. 3, pp. 212–243, 2020.
- [21] S. Vummadisetti and S. B. Singh, "Postbuckling response of functionally graded hybrid plates with cutouts under in-plane shear load," *Journal of Building Engineering*, vol. 33, Article ID 101530, 2021.
- [22] S. Vummadisetti and S. B. Singh, "Boundary condition effects on postbuckling response of functionally graded hybrid composite plates," *J. Struct. Eng. SERC*, vol. 47, no. 4, pp. 1–17, 2020.
- [23] Standard, Astm, *Standard Test Method for Tensile Properties of Polymer Matrix Composite Materials*, ASTM D3039/D M 3039, Conshohocken, PA, USA, 2008.
- [24] S. B. Singh, S. Vummadisetti, and H. Chawla, "Influence of curing on the mechanical performance of FRP laminates," *Journal of Building Engineering*, vol. 16, pp. 1–19, 2018.
- [25] Astm, International, *Standard Test Methods for Flexural Properties of Unreinforced and Reinforced Plastics and Electrical Insulating Materials*, ASTM D790–07, Conshohocken, PA, USA, 2007.